Topological Superconductivity in Twisted Multilayer Graphene

Cenke Xu[1] and Leon Balents[2]

[1]*Department of Physics, University of California, Santa Barbara, California 93106, USA*
[2]*Kavli Institute of Theoretical Physics, Santa Barbara, California 93106, USA*

We study a minimal Hubbard model for electronically driven superconductivity in a correlated flat miniband resulting from the superlattice modulation of a twisted graphene multilayer. The valley degree of freedom drastically modifies the nature of the preferred pairing states, favoring spin triplet $d + id$ order with a valley singlet structure. We identify two candidates in this class, which are both *topological* superconductors. These states support half-vortices carrying half the usual superconducting flux quantum $hc/(4e)$, and have topologically protected gapless edge states.

Recent experiments [1–3] demonstrate remarkable correlation phenomena in twisted multilayer graphene with small twist angles, for which the resulting moiré pattern induces an effective triangular superlattice with a unit cell much larger than the microscopic one. The superlattice generally induces minibands with a reduced superlattice Brillouin zone. It was theoretically predicted that flat minibands should exist in such systems, an effect especially pronounced near "magic angles" in bilayer systems [4–7]. When the miniband at the Fermi energy is much narrower than the effective Coulomb interaction energy per electron, then correlation effects may be expected. Experiments on bilayers [1] and trilayers [3] find evidence for a correlated Mott insulating state when such a miniband contains an integer number of electrons per superlattice unit cell. Furthermore, gate tuning the charge density away from the half-filling bilayer moiré Mott insulator with 2 electrons per unit cell led to superconductivity with strong coupling characteristics [2]. Many features are strikingly similar to those of the cuprate high-T_c materials, for which superconductivity also occurs in close proximity to a Mott insulator. This raises the intriguing possibility of graphene moiré superlattices serving as a new platform for unconventional superconductivity with unprecedented *in situ* tunability. The goal of the current work is to understand the nature of the observed superconducting phases. We argue that even in the simplest situation, the valley degree of freedom (d.o.f.) of graphene leads to dramatic modifications to the superconductivity: the preferred states are *topological* superconductors with a valley singlet structure.

Our results are based on the minimal description of a correlated flat band in terms of a Hubbard model, with a single "site" per unit cell. This is valid when the superlattice period is large, and when the interband mixing may be neglected. For such a flat band, the (weak) tunneling between nearest-neighbor unit cells dominates the kinetic energy. The large period suppresses interactions beyond nearest-neighbor sites. Furthermore, each unit cell effectively hosts two degenerate orbital wave functions for electrons, which correspond to the two original valleys at the Brillouin zone corners, since the large unit cell moiré modulation cannot mix these states due to their large momentum space separation. Our starting point is therefore a two-orbital Hubbard model on the triangular lattice, with in total four flavors of single-electron states on each site, including both the spin and orbital d.o.f.:

$$H = -t \sum_{\langle ij \rangle} \sum_{\alpha=1}^{4} (c_{i,\alpha}^{\dagger} c_{j,\alpha} + \text{H.c.}) + U \sum_{j} \left(\sum_{\alpha=1}^{4} n_{j,\alpha} \right)^2. \quad (1)$$

Equation (1) has an SU(4) symmetry which corresponds to the rotation between the four flavors of electron states.

This symmetry is justified as follows. For the hopping term, SU(2) spin-rotation invariance requires the hopping to be spin independent. Mixing between different orbital states is prohibited by the large valley separation in momentum space. The reality and equality of the nearest neighbor hopping amplitudes for the two different orbitals follows, at least for twisted bilayer graphene (Fig. 1), by careful consideration of $2\pi/3$ rotation, reflection $y \rightarrow -y$ (which exchanges the valleys) and reflection $x \rightarrow -x$. Thus with only nearest neighbor hoppings, the SU(4) symmetry of the hopping term in Eq. (1) should be an excellent approximation [8]. The SU(4) symmetry of the U term follows from its dependence only on the *total* charge of a site, which physically represents the capacitive energy of a superlattice unit cell due to "medium range" Coulomb interactions, i.e., on scales large compared to the microscopic lattice spacing, but small compared to the screening length. Corrections to this SU(4) symmetry arising from short-range interactions do exist and will be considered later, but are weaker than the dominant SU(4) part by a
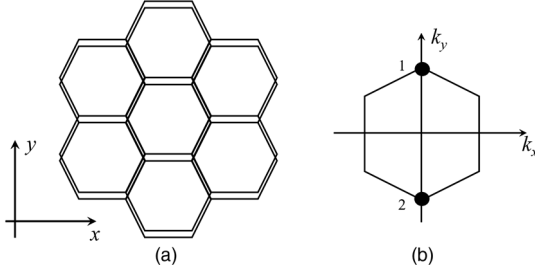
FIG. 1. (a) The center of a unit cell of a bilayer graphene moiré superlattice, where Wannier states are peaked in the flat band. In this region there is AA stacking of the two layers, and coordinates referred to in the text are defined as shown. (b) Independent single-particle states are built from momenta near each of the two valleys shown as dark dots in the microscopic Brillouin zone corners, and these become the two orbitals in the Hubbard model of Eq. (1).

factor proportional to a/a_0, where a is the superlattice spacing and a_0 is the microscopic lattice spacing.

When the number of electrons per site of Eq. (1) is $\bar{n} = 1, 2$, or 3, and when U/t is sufficiently large, the system becomes a Mott insulator. An effective SU(4) Heisenberg model for the Mott insulator can be derived using the standard perturbation theory based on the Hubbard model Eq. (1):

$$H_J = J\sum_{\langle ij \rangle} \sum_{a=1}^{15} \hat{T}_i^a \hat{T}_j^a, \qquad (2)$$

where $\hat{T}_i^a = c_{i,\alpha}^\dagger T_{\alpha\beta}^a c_{i,\beta}$, $c_{i\alpha}^\dagger c_{i\alpha} = \bar{n}$ and $T_{\alpha\beta}^a$ with $a = 1, \ldots, 15$ are fifteen 4×4 Hermitian matrices that form the fundamental representation of the SU(4) Lie-algebra (we choose $\mathrm{Tr} T^a T^b = 4\delta^{ab}$). The SU(4) spin model Eq. (2) itself is already an interesting subject to study, and compared with SU(2) spin systems, it is more likely to support exotic spin liquid ground states [9–20]. But in this work we will focus on the superconductor phase next to the Mott insulator after doping.

The Heisenberg interaction in Eq. (2) can be rewritten in a different form (a Fierz identity [21]):

$$H_J = J\sum_{\langle ij \rangle} \left[-\frac{5}{4}(\vec{\Delta}_{ij})^\dagger \cdot \vec{\Delta}_{ij} + \frac{3}{4}(\Delta_{ij}^-)^\dagger \cdot \Delta_{ij}^- \right], \qquad (3)$$

where we defined the 6 component $\vec{\Delta}_{ij} = \vec{\Delta}_{ji}$ and 10 component $\Delta_{ij}^- = -\Delta_{ji}^-$ pairing fields symmetric and antisymmetric, respectively, in $i \leftrightarrow j$. Obviously, the antiferromagnetic interactions ($J > 0$) appropriate near half-filling favor condensing the operators $\vec{\Delta}_{ij}$, which are "even parity" in this sense, and we henceforth neglect the odd parity channel. In fact, $\vec{\Delta}_{ij}$ transforms as an SO(6) vector [SU(4)~ SO(6)], when written in an appropriate basis:

$$\vec{\Delta}_{ij} = c_i^t(\sigma^{32}, i\sigma^{02}, \sigma^{12}, i\sigma^{23}, \sigma^{20}, i\sigma^{21})c_j, \qquad (4)$$

where $\sigma^{ab} = \sigma^a \otimes \sigma^b$, $\sigma^0 = \mathbf{1}_{2\times2}$. The first and second Pauli matrices in the tensor product operate on the spin and valley spaces, respectively. The six-component vector Δ^a can be decomposed into a three component spin-triplet and orbital-singlet pairing vector $\Delta = (\Delta^1, \Delta^2, \Delta^3)$, and another three component spin-singlet and orbital-triplet pairing vector $(\Delta^4, \Delta^5, \Delta^6)$. With the SU(4) symmetry of Eqs. (1) and (2), these two sets of three-component vectors are exactly degenerate.

Upon doping (for instance, hole doping), one can turn on a kinetic term on Eq. (3), and the large U limit becomes a t-J model with a projection that prohibits more than two particles per site. In an intermediate coupling scenario we can simply add H_J to the Hamiltonian to represent the effects of antiferromagnetic fluctuations. Then a standard mean field theory leads to a condensate of $\vec{\Delta}_{ij}$, i.e., superconductivity. Because of Fermi statistics, this even parity pairing is antisymmetric in SU(4) flavor space, which is the essence of superexchange that favors antiferromagnetism. Amongst the even parity channels, s-wave pairing is penalized by the large on-site Hubbard U interaction, and we expect d-wave pairing to be favored. Previous studies for SU(2) superconductors on the triangular lattice found that, to ensure the entire Fermi surface is gapped, $d_{x^2-y^2} + id_{xy}$ pairing is often favored [22–28].

Now let us consider the effects of SU(4) symmetry-breaking perturbations to the Hubbard model. Significant effects arise from interactions, which are analogous to Kanamori terms multiorbital Hubbard systems. As is usually the case for transition metal ions, we assume that the most important of these is the Hunds coupling

$$H_h = -V\sum_j (\mathbf{S}_j)^2, \qquad (5)$$

where $V > 0$ and $\mathbf{S}_j$ is the total spin on site j. The Hunds coupling H_h is expected to further prefer the three-component spin-triplet and orbital singlet pairing vector $\vec{\Delta}$ over the other three components of the SO(6) vector $\vec{\Delta}$. To see this, consider two nearest neighbor sites that are both doped with one hole; i.e., each site is occupied by one electron, at second order perturbation theory in t/U. Suppose the two electrons form a spin-singlet and orbital-triplet state, then the virtual intermediate state contains one doubly occupied site which increases the energy relative to two singly occupied sites by $2U$; while if the two electrons form a spin-triplet state, then the virtual intermediate state has energy $2U - 2V$, which is lower than the previous case due to the Hunds interaction Eq. (5) (Fig. 2). Thus the Hunds coupling will select the spin-triplet and orbital-singlet components from the SO(6) vector $\vec{\Delta}$, and the energy splitting is at the order of
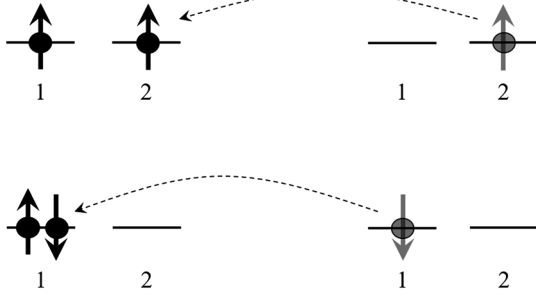
FIG. 2. The virtual process in second order perturbation theory in t/U. An electron hops from the singly occupied site on the right to the one on the left, making it doubly occupied. The intermediate state may be (top) a spin triplet and orbital singlet or (bottom) a spin singlet and orbital triplet. The Hunds interaction favors the upper situation.

$\sim t^2/(2U-2V) - t^2/(2U) \sim Vt^2/(2U^2)$. The analysis of the electron-doped case leads to the same conclusion. Instead of the two site argument, one may alternatively just consider the modification of the super-exchange interaction of Eq. (3) by the V term. This leads to a ferromagnetic contribution purely in the spin sector $\sim -J(V/U)\sum_{\langle ij\rangle}S_i \cdot S_j$, which by a similar Fierz identity favors triplet pairing.

It is noteworthy that the valley d.o.f. allows the formation of an even parity (d-wave) spin-triplet state, which is impossible due to Fermi statistics for a single orbital model. Here it occurs because the orbital singlet is antisymmetric. However, in our discussion we defined the parity and angular momentum of the pair with respect to the two-orbital Hubbard model. Microscopically, parity also exchanges the two valleys, so in terms of the large microscopic Brillouin zone, the even parity d-wave state becomes an odd-parity f-wave one. We stick with the former convention for concreteness.

Knowing that the system favors spin-triplet $d + id$ or $d \pm id$ pairing, most generally we can write the spin-triplet Cooper pair matrix in the BdG Hamiltonian as

$$\Delta_{\boldsymbol{k}} = (u_k \Phi_1 + v_k \Phi_2) \cdot i\sigma^2 \boldsymbol{\sigma} \otimes \sigma^2, \qquad (6)$$

where $u_k = \cos k_x - \cos(k_x/2)\cos(\sqrt{3}k_y/2)$ and $v_k = \sqrt{3}\sin(k_x/2)\sin(\sqrt{3}k_y/2)$ are the periodic superlattice analogs of the $k_x^2 - k_y^2$ and $2k_x k_y$ pairing functions, respectively. Here Φ_1 and Φ_2 are both *complex* SO(3) spin vectors. To minimize the energy and maximize the pairing gap on the Fermi surface, there are two candidate states that are degenerate at the mean field level:

$$A: \quad \Phi_2 = i\Phi_1 = i\phi e^{i\theta},$$
$$B: \quad \Phi_1 = \phi_1 e^{i\theta}, \qquad \Phi_2 = \phi_2 e^{i\theta}. \qquad (7)$$

Here ϕ, ϕ_1, ϕ_2 are all three-component real vectors under spin SO(3) rotation, and $\phi_1 \cdot \phi_2 = 0$. Other types of spin-triplet superconductors, for example, $\Delta_{\boldsymbol{k}} \sim (u_k + iv_k)(\phi_1 + i\phi_2)$, with real vectors $\phi_1 \cdot \phi_2 = 0$, do not have a uniform maximal gap on the Fermi surface, and are thus less favorable within mean field theory than types A and B.

Type A and B states are degenerate within the standard BCS mean field theory. This is apparent from comparing for example the type A state with $\phi \sim (0,1,0)$ and the type B state $\phi_1 \sim (1,0,0)$ and $\phi_2 \sim (0,1,0)$. In the former, both spin-up and spin-down electrons experience $d + id$ pairing, while in the latter, the pair field for up spin electrons is $d + id$, and the pair field for down electrons is $d - id$. The gap magnitudes are everywhere identical in the two cases, and hence they have the same mean field energy. This is the consequence of an artificial symmetry in the mean field formalism: a reflection symmetry $k_x \to -k_x$ on spin down electrons only, which interchanges the two types of pairings. Taking the most general form of the pairing order parameter $\Phi_{\vec{k}} = (u_k \Phi_1 + v_k \Phi_2)$ with complex vectors Φ_1, Φ_2, the BCS mean field theory generates a Landau-Ginzburg free energy

$$F = \sum_{\vec{k}} r|\Phi_{\vec{k}}|^2 + g(|\Phi_{\vec{k}}|^2)^2 - c|\Phi_{\vec{k}} \cdot \Phi_{\vec{k}}|^2. \qquad (8)$$

The last term maintains the degeneracy between type A and type B pairing, but disfavors other types of pairings. In general, effects beyond the BCS treatment will generate additional terms in the Landau-Ginzburg free energy and lift the degeneracy between type A and B. We will not attempt to resolve which state is favored here, but simply discuss the properties of both candidate states.

Consider time-reversal symmetry, which flips spin *and* exchanges the two valleys, hence $c \to \sigma^{21}c$. It also induces complex conjugation, so it acts on the order parameter $\Phi_{\vec{k}}$ as $\mathcal{T}: \Phi_{\vec{k}} \to \Phi^*_{-\vec{k}}$. Thus type A pairing breaks time-reversal symmetry because $u_k + iv_k \to u_k - iv_k$ under complex conjugation, while type B pairing is time-reversal invariant.

Now consider the topology of the order parameter. Within a single time-reversal sector, the type A state has the ground state manifold $[S^2 \times S^1]/Z_2$. Here S^2 corresponds to the configuration of the spin SO(3) vector ϕ, S^1 corresponds to the configuration of $e^{i\theta}$. The full order parameter is invariant under a Z_2 transformation

$$\phi \to -\phi, \qquad \theta \to \theta + \pi. \qquad (9)$$

Because of this, type A pairing supports a half-vortex, analogous to that in the polar state of spin-1 bosons in cold atom systems [29–31]. After tracing along a full circle around the half-vortex core, both ϕ and $e^{i\theta}$ acquire a minus sign (while Δ remains single valued). The half-vortex carries a quantized magnetic flux

$$\Phi_0 = \frac{hc}{4e}, \tag{10}$$

which is half of the magnetic flux quantum of ordinary superconductors. Moreover, as was discussed in Ref. [31], in this purely two-dimensional superconductor, the Mermin-Wagner theorem dictates that SO(3) vector $\boldsymbol{\phi}$ is disordered at infinitesimal temperature due to thermal fluctuations. Hence the system no longer has long-range or even quasi-long-range order of Δ. Instead, what persists are power-law correlations of a spin-singlet charge-$4e$ order parameter $\Delta \cdot \Delta \sim e^{2i\theta}$. The Kosterlitz-Thouless transition out of this algebraic charge-$4e$ superconducting phase is driven by unbinding of half-vortices, which leads to a universal superconductor phase stiffness jump $8T_c/\pi$ at the transition [31].

While type B pairing does not break time-reversal symmetry, it has similar finite temperature behavior. The vectors ϕ_1 and ϕ_2 are disordered immediately by infinitesimal temperature, and the system effectively becomes an algebraic charge-$4e$ superconductor with a half-vortex that carries $hc/(4e)$ magnetic flux.

Both type A and type B superconductors are topological, in the sense that they both have gapless edge states at their boundary. In the type A superconductor, the boundary has eight channels of chiral Majorana fermions, which in the ideal case leads to a thermal Hall conductance

$$\kappa_{xy} = \frac{4\pi^2 k_B^2 T}{3h}. \tag{11}$$

The edge states of the type A superconductor are stable against any disorder and interaction because they are chiral and hence no backscattering can occur. In the type A superconductor, because the spin symmetry is spontaneously broken down to U(1), one spin component is still conserved: for $\phi \sim (0,0,1)$, this is S^z. In this case, it is convenient to introduce a new basis of fermion, for orbital (valley) 1, define $\psi_{\alpha,1} = c_{\alpha,1}$; for orbital 2, define $\psi_{\alpha,2} = \sigma^2_{\alpha\beta}c^\dagger_{\beta,2}$, $\alpha, \beta = \uparrow, \downarrow$. Then the entire mean field Bogoliubov–de Gennes Hamiltonian for quasiparticles reads

$$\hat{H} = \sum_{\vec{k}} \psi^\dagger_{\vec{k}} \mathcal{H}(\vec{k}) \psi_{\vec{k}},$$
$$\mathcal{H}(\vec{k}) = \epsilon_k \sigma^{03} + \Delta(u_k \sigma^{31} + v_k \sigma^{32}). \tag{12}$$

In this basis, spin-up and spin-down fermions $\psi_\uparrow$, $\psi_\downarrow$ both have Hall conductivity $\sigma_{xy} = 2$, which is visible in Eq. (12) because the pair field acts in the orbital space (second index ν of $\sigma^{\mu\nu}$) as a vector in the 1–2 plane which winds twice around the origin in momentum space. Hence the eight channels of chiral Majorana fermion edge states can be reorganized into two channels of chiral edge states each for

$\psi_\uparrow$ and $\psi_\downarrow$. Thus the system also has a "spin quantum Hall" conductance $\sigma^s_H = 4$: namely, if we couple the system to a "spin gauge field" A^s_μ, and spin-up, spin-down electrons carry gauge charge ± 1 under the spin gauge field A^s_μ, then after integrating out all the fermions, the system generates a level-4 Chern-Simons term for the background spin gauge field: $\mathcal{L}_{cs} = (4/4\pi)\epsilon_{\mu\nu\rho}A^s_\mu \partial_\nu A^s_\rho$.

In the type B superconductor, the boundary has four channels of counterpropagating nonchiral Majorana fermions, and there is no thermal Hall effect. The stability of the edge states of type-B superconductor deserves a bit more discussion. Let us again take $\phi_1 \sim (1,0,0)$, and $\phi_2 \sim (0,1,0)$, then this superconductor can be simply viewed as spin-up electrons and spin-down electrons forming $d+id$ and $d-id$ topological superconductors separately, and its edge state Hamiltonian reads

$$H_{1d} = \int dx \sum_{\alpha=1}^4 \chi_{L,\alpha} i\partial_x \chi_{L,\alpha} - \chi_{R,\alpha} i\partial_x \chi_{R,\alpha}. \tag{13}$$

The order of ϕ_1 and ϕ_2 fully breaks SO(3) spin symmetry, while the Z_2 symmetry in Eq. (9) (a product of π rotation in the spin and charge sectors) is preserved. The Z_2 symmetry acts on the quasiparticles of the superconductor as a fermion parity for the right-moving fermion $\chi_{R,\alpha}$ only: $\chi_{L,\alpha} \to \chi_{L,\alpha}$, $\chi_{R,\alpha} \to -\chi_{R,\alpha}$, which also prohibits any mixing between left and right moving modes. Without interactions, the classification of this topological superconductor is obviously $\mathbb{Z}$. Even including interactions that preserve this Z_2 symmetry, the edge state in Eq. (13) with four channels of nonchiral Majorana fermions is still topologically stable, namely, it cannot be gapped out without breaking the Z_2 symmetry [32–37].

In this work we considered electronically driven superconductivity in graphene moiré superlattices within a minimal single band triangular lattice Hubbard model with spin + orbital degeneracy. We found that the valley d.o.f. of graphene has qualitative effects on the superconductivity compared to single-orbital Hubbard systems. Standard Hund's coupling favors topological $d+id$ paired spin-triplet states. With SU(2) spin-rotation symmetry, these states support exotic charge $4e$ pairing and half-vortices at nonzero temperature. Thus graphene may become not only a venue for strong correlation physics, but also topological superconductivity.

Subsequent to the posting of the first version of this Letter, a number of papers appeared emphasizing the physics related to Dirac band crossings between a *pair* of flat minibands appearing in some models of the moiré superlattice [38,39]. In this situation the two low energy bands are intertwined and there is no obvious separation between them. Consequently, in the strong coupling limit, the minimal description is two band honeycomb lattice model, for which both the kinetic energy and interactions

are more complicated than in Eq. (1). In the intermediate correlation regime, states near the Fermi energy dominate the superconductivity, and it is not clear that either the additional band far from the Fermi energy or any symmetry protected Dirac point plays a major role. The weak activation gap in the MI phase does suggests that the system only has an at most intermediate correlation effect. We suggest that future experiments which monitor the superconductivity while at the same time inducing a measurable gap at the Dirac crossing would be highly desirable, because they can directly test whether band topology is actually relevant to the correlation physics.

The major difference between Ref. [38] and our own work is that the former invokes [SU(4)] ferromagnetism, while we rely upon the effective anti-ferromagnetic interaction, Eq. (2). However, ferromagnetism in Hubbard models is notoriously hard to find, and antiferromagnetism may be more robust even when the honeycomb description is more appropriate. The compelling simplicity of the triangular framework suggests that graphene moiré heterostructures which realize the single band triangular regime are favorable for realizing topological physics. This constitutes a design goal which is realizable theoretically and experimentally.

Further studies should address these states quantitatively, the possibility of quantum spin liquid physics in the Mott states, and the effects of perturbations to the minimal Hubbard description such as second neighbor hopping, disorder, magnetic fields, and more. The low energy scale of these graphene superlattices allows vastly larger tuning of doping and magnetic field axes in comparison to conventional correlated transition metal compounds, and their pure two dimensionality makes probing strictly Zeeman effects also possible. Our results may serve as guidance for such future studies.

---

[1] Y. Cao, V. Fatemi, A. Demir, S. Fang, S. L. Tomarken, J. Y. Luo, J. D. Sanchez-Yamagishi, K. Watanabe, T. Taniguchi, E. Kaxiras *et al.*, Nature (London) **556**, 80 (2018).

[2] Y. Cao, V. Fatemi, S. Fang, K. Watanabe, T. Taniguchi, E. Kaxiras, and P. Jarillo-Herrero, Nature (London) **556**, 43 (2018).

[3] G. Chen, L. Jiang, S. Wu, B. Lv, H. Li, K. Watanabe, T. Taniguchi, Z. Shi, Y. Zhang, and F. Wang, arXiv: 1803.01985.

[4] R. Bistritzer and A. H. MacDonald, Proc. Natl. Acad. Sci. U.S.A. **108**, 12233 (2011).

[5] E. Suárez Morell, J. D. Correa, P. Vargas, M. Pacheco, and Z. Barticevic, Phys. Rev. B **82**, 121407 (2010).

[6] S. Fang and E. Kaxiras, Phys. Rev. B **93**, 235153 (2016).

[7] G. Trambly de Laissardière, D. Mayou, and L. Magaud, Phys. Rev. B **86**, 125413 (2012).

[8] The (postulated) microscopic symmetry of the system allows valley-dependent imaginary second neighbor hopping, with which the Fermi surface of the system can be very faithfully captured. In the current work we consider the minimal version of the model, with only nearest-neighbor hoppings. Perturbations by the second neighbor hopping do not change the conclusions of the Letter.

[9] C. Wu, J.-p. Hu, and S.-c. Zhang, Phys. Rev. Lett. **91**, 186402 (2003).

[10] C. Wu, Phys. Rev. Lett. **95**, 266404 (2005).

[11] C. Xu and C. Wu, Phys. Rev. B **77**, 134449 (2008).

[12] M. Hermele and V. Gurarie, Phys. Rev. B **84**, 174441 (2011).

[13] L. Savary, arXiv:1511.01505.

[14] M. Hermele, V. Gurarie, and A. M. Rey, Phys. Rev. Lett. **103**, 135301 (2009).

[15] M. Hermele, T. Senthil, and M. P. A. Fisher, Phys. Rev. B **72**, 104404 (2005).

[16] A. Mishra, M. Ma, and F.-C. Zhang, Phys. Rev. B **65**, 214411 (2002).

[17] A. V. Gorshkov, M. Hermele, V. Gurarie, C. Xu, P. S. Julienne, J. Ye, P. Zoller, E. Demler, M. D. Lukin, and A. M. Rey, Nat. Phys. **289**, 6 (2010).

[18] R. K. Kaul, Phys. Rev. B **84**, 054407 (2011).

[19] M. G. Yamada, M. Oshikawa, and G. Jackeli, arXiv:1709.05252.

[20] W. M. H. Natori, E. C. Andrade, and R. G. Pereira, arXiv:1802.00044.

[21] L. Savary, J. Ruhman, J. W. F. Venderbos, L. Fu, and P. A. Lee, Phys. Rev. B **96**, 214514 (2017).

[22] Q.-H. Wang, D.-H. Lee, and P. A. Lee, Phys. Rev. B **69**, 092504 (2004).

[23] S. Zhou and Z. Wang, Phys. Rev. Lett. **100**, 217002 (2008).

[24] K. S. Chen, Z. Y. Meng, U. Yu, S. Yang, M. Jarrell, and J. Moreno, Phys. Rev. B **88**, 041103 (2013).

[25] T. Watanabe, H. Yokoyama, Y. Tanaka, and J. ichiro Inoue, Physica (Amsterdam) **463–465C**, 152 (2007).

[26] C. Weber, A. Läuchli, F. Mila, and T. Giamarchi, Phys. Rev. B **73**, 014519 (2006).

[27] T. Watanabe, H. Yokoyama, Y. Tanaka, J. ichiro Inoue, and M. Ogata, J. Phys. Chem. Solids **67**, 95 (2006).

[28] T. Watanabe, H. Yokoyama, Y. Tanaka, J. ichiro Inoue, and M. Ogata, J. Phys. Soc. Jpn. **73**, 3404 (2004).

[29] T.-L. Ho, Phys. Rev. Lett. **81**, 742 (1998).

[30] T. Ohmi and K. Machida, J. Phys. Soc. Jpn. **67**, 1822 (1998).

[31] S. Mukerjee, C. Xu, and J. E. Moore, Phys. Rev. Lett. **97**, 120406 (2006).

[32] L. Fidkowski and A. Kitaev, Phys. Rev. B **81**, 134509 (2010).

[33] L. Fidkowski and A. Kitaev, Phys. Rev. B **83**, 075103 (2011).

[34] S. Ryu and S.-C. Zhang, Phys. Rev. B **85**, 245132 (2012).

[35] X.-L. Qi, New J. Phys. **15**, 065002 (2013).

[36] H. Yao and S. Ryu, Phys. Rev. B **88**, 064507 (2013).

[37] Z.-C. Gu and M. Levin, Phys. Rev. B **89**, 201113 (2014).

[38] H. C. Po, L. Zou, A. Vishwanath, and T. Senthil, arXiv:1803.09742.

[39] N. F. Yuan and L. Fu, Phys. Rev. B **98**, 045103 (2018).